

The directed flow maximum near $c_s = 0$

J. Brachmann¹, A. Dumitru², H. Stöcker¹, W. Greiner¹

¹Institut für Theoretische Physik der J.W. Goethe-Universität
Postfach 111932, D-60054 Frankfurt am Main, Germany

²Physics Department, Columbia University
704 Pupin Hall, 538W 120th Street, New York, NY 10027, USA

November 1999

We investigate the excitation function of quark-gluon plasma formation and the rapidity dependence of directed in-plane flow of nucleons in the energy range of the BNL-AGS and for the $E_{Lab}^{kin} = 40A$ GeV Pb+Pb collisions performed recently at the CERN-SPS. We employ the three-fluid model with dynamical unification of kinetically equilibrated fluid elements. Within our model with first-order phase transition at high density, droplets of QGP co-existing with hadronic matter are produced already at BNL-AGS energies, $E_{Lab}^{kin} \simeq 10A$ GeV. A substantial decrease of the isentropic velocity of sound, however, requires higher energies, $E_{Lab}^{kin} \simeq 40A$ GeV. We calculate the response of the directed in-plane momentum per nucleon, $\langle p_x/N \rangle(y)$. According to our model calculations, kinematic requirements and EoS effects work hand-in-hand at $E_{Lab}^{kin} = 40A$ GeV to allow the observation of the dropping velocity of sound and of the “slowly burning” mixed phase via an *increase* of the directed flow around midrapidity as compared to top BNL-AGS energy.

The theory of strong interactions, QCD, exhibits a thermodynamical phase transition to a so-called quark-gluon plasma (QGP) at high energy density [1]. To achieve densities far beyond that of the nuclear ground state one collides heavy ions at high energies [2–7]. If the equation of state (EoS) exhibits no anomalous structure, one expects that the volume and life-time of the QGP increase with energy.

Due to non-equilibrium effects, however, higher impact energies do not necessarily yield a larger amount of energy deposition in the central region. One-fluid dynamical calculations of the compression neglect initial non-equilibrium processes and predict sharp signals for the phase transition to the QGP [2–7]. How strongly these predictions are washed out by non-equilibrium effects has to be investigated via excitation functions. Therefore, the energy range from BNL-AGS energies ($2 - 11A$ GeV) to CERN-SPS energies (previously only $160 - 200A$ GeV) is highly interesting to study the EoS of nuclear matter, and possibly the onset of QGP formation. In particular, data at $40A$ GeV has been taken recently at the CERN-SPS to complete the already existing data [8–10] on the excitation function of collective flow.

Motivated by the fact that the proton rapidity distribution in high energy pp reactions is strongly forward-backward peaked [11], we developed a fluid-dynamical model in which the projectile and target nucleons constitute *distinct* fluids. The coupling between those fluids is obtained from a parametrization of free binary NN collisions [12], which leads to a gradual deceleration. The three-fluid model [13,14] also considers the newly produced particles around midrapidity as a distinct fluid which we call “fireball”. This appears reasonable since they populate a distinct rapidity region as well (at early times!). The assumption of local equilibrium is imposed within each fluid, but the total energy-momentum tensor does *not* need to be that of an ideal fluid.

However, after several collisions projectile and target nucleons are stopped, and local thermal equilibrium establishes between projectile and fireball fluid or between target and fireball fluid, respectively, and finally for all three fluids. The respective fluids i and j are then unified by adding their energy-momentum tensors and net-baryon currents at the corresponding space-time point, $T_i^{\mu\nu}(x) + T_j^{\mu\nu}(x) = T_{\text{unified}}^{\mu\nu}(x)$, $N_i^\mu(x) + N_j^\mu(x) = N_{\text{unified}}^\mu(x)$. Common values for e , p , ρ and $u^\mu \equiv \gamma(1, \mathbf{v})$ are then obtained from $T_{\text{unified}}^{\mu\nu} = (e + p) u^\mu u^\nu - p g^{\mu\nu}$ and $N_{\text{unified}}^\mu = \rho u^\mu$, and the given EoS $p = p(e, \rho)$. The local criterion for unification employed here is $(p_i + p_j)/p > 0.9$, i.e. the sum of the individual pressures p_i and p_j of fluids i and j , respectively, is compared to the total pressure p in equilibrium. The dynamical unification allows friction-free ideal expansion of equilibrated fluids.

The model calculation starts with two nuclei in the ground state and treats the compression (deceleration) stage as well as the subsequent expansion. The fluid-dynamical equations are solved in 3+1 dimensions, cf. [13] for details. The EoS employed here exhibits a first order phase transition to a QGP [6]. The hadronic phase consists of nucleons interacting via exchange of σ and ω mesons [15], plus thermal pions. The QGP phase is described in the

framework of the MIT-Bag model [16] as an ideal gas of u and d quarks and gluons, with a bag parameter $B^{1/4} = 235$ MeV, resulting in a critical temperature $T_c \simeq 170$ MeV at $\rho = 0$. The first order phase transition is constructed via Gibbs' conditions of phase coexistence.

Fig. 1 shows the average isentropic velocity of sound and the fraction of baryon charge in each phase at various energies. Spectators were discarded in the latter analysis. Throughout the manuscript, averages on fixed CM-time hypersurfaces employ the time-like component of the net-baryon four-current as the weight-function.

The formation of plasma droplets starts already at BNL-AGS energies. However, the baryon density ρ in this energy domain is large and $\langle c_s \rangle$ is not very small. Thus, the response of the highly excited matter to energy density gradients is *not* weak at these BNL-AGS energies. However, at the higher CERN-SPS energies, $E_{Lab}^{kin} \geq 40A$ GeV, an extended time-interval where $\langle c_s \rangle$ is small *does* exist.

Fig. 1 also shows the slow rehadronization of mixed phase at $E_{Lab}^{kin} \geq 40A$ GeV. (However, around $y = 0$ the fluid does hadronize within the depicted time interval.) In contrast to this interesting prediction of fluid dynamics, cf. also [6,7,17], the excitation function of entropy production increases monotonically with energy, and exhibits no “anomalous” structure [18]. Note also that non-equilibrium effects in the early stage of the reaction limit the gain of QGP; it does not increase dramatically from $E_{Lab}^{kin} = 40A$ GeV to $160A$ GeV.

The EoS $p = p(e, \rho)$ is usually investigated by studying various flow patterns [5–7,19–24]. We shall discuss here how the directed in-plane flow, formerly called the *bounce-off* [3,9], “responds” to the behavior of $\langle c_s \rangle$. The pressure in the overlap zone deflects the colliding nuclei. Directed flow can be investigated in terms of the mean in-plane momentum per nucleon as a function of rapidity $y \equiv \text{Artanh } v_z$ [20]. We decompose the flow as [24]

$$\left\langle \frac{p_x^{\text{flow/antiflow}}}{N} \right\rangle (t, y) \equiv \frac{\int_y d^3 \mathbf{x} N^0(t, \mathbf{x}) m_N u_x(t, \mathbf{x}) \theta[\pm y p_x(t, \mathbf{x})]}{\int_y d^3 \mathbf{x} N^0(t, \mathbf{x})} . \quad (1)$$

The subscript on the integral indicates that the integration extends only over fluid elements with rapidity y ; thermal and Fermi-momenta are neglected. v_x, v_z are the components of the velocity field parallel to the impact parameter vector, and to the beam axis, respectively.

The sum of the two flow components, $\langle p_x/N \rangle \equiv \langle p_x^{\text{flow}}/N \rangle + \langle p_x^{\text{antiflow}}/N \rangle$, usually exhibits an S-shape [3,9,20,21] because projectile nucleons at positive rapidities are deflected into the positive x -direction, and vice versa for target matter. However, a variety of experimental data [8,10] as well as theoretical investigations [5,6,22] show deviations from the S-shaped $\langle p_x/N \rangle(y)$. One rather observes a plateau or even a reversed flow (negative slope) in the midrapidity region, at least if viscous effects are not dominant. That plateau is related to the geometrical shape of the high-density region in coordinate space [23,24].

At $E_{Lab}^{kin} = 2A$ GeV, one observes ordinary (positive) directed flow, cf. Fig. 2. Towards the end of the reaction $\langle p_x/N \rangle(y)$ has positive and clearly non-zero slope near midrapidity. This behavior changes when the energy is increased. Fig. 3 shows that at $E_{Lab}^{kin} \simeq 8A$ GeV the

above-mentioned plateau near midrapidity occurs, which eventually even turns into reversed flow [22–24]. It is due to the expansion into the direction orthogonal to the normal directed flow, resulting from the tilt of the hot and dense region in the reaction plane [24]. Obviously, the expansion into the “anti-flow” direction can only build up because $\langle c_s \rangle$ is *not* small.

At $E_{Lab}^{kin} = 40A$ GeV, $\langle c_s \rangle$ is less than 0.2 when the phase coexistence region is reached from above and the “slow burning” of the mixed phase [6,7,17] sets in, cf. Fig. 1. This *prevents* build-up of anti-flow and “cancellation” of the positive flow, cf. Fig. 4. Integrating $\langle p_x/N \rangle(y)$ over rapidity leads to a maximum of p_x^{dir}/N around $E_{Lab}^{kin} = 40A$ GeV [24].

At even higher energies, $E_{Lab}^{kin} = 160A$ GeV and more, $\langle p_x/N \rangle(y)$ becomes flat again (around midrapidity) for purely kinematical reasons [6,21,24], as can also be observed in the data [10]. That behavior is rather insensitive to the EoS.

In summary, we investigated the excitation function of QGP formation in relativistic heavy-ion collisions. We find that droplets of QGP coexisting with hadronic matter are already produced at the top BNL-AGS energy, $E_{Lab}^{kin} \simeq 10A$ GeV. However, the average speed of sound in the dense baryonic matter does not drop very much, even in case of a first-order phase transition. As a consequence, expansion of matter is not inhibited and anti-flow develops, diminishing the net directed flow more and more as beam energy increases towards top BNL-AGS energy. This is qualitatively consistent with experimental results obtained for Au+Au collisions at $E_{Lab}^{kin} = 2 - 10A$ GeV [8].

Furthermore, we showed that the forthcoming results of the Pb+Pb reactions at $E_{Lab}^{kin} = 40A$ GeV will test whether the picture of hot QCD-matter as a heat-bath with small isentropic speed of sound (mixed phase) is indeed applicable to heavy-ion collisions in this energy domain. *If* it holds true, our model calculation predicts that the slope of $\langle p_x/N \rangle(y)$ around midrapidity increases considerably as compared to top BNL-AGS energy; pressure gradients along isentropes are so small that the anti-flow can not develop and the regular positive flow can not be cancelled. Thus, those reactions can shed light on the (non-?)existence of a local maximum of directed flow, related to a substantial decrease of the isentropic speed of sound.

ACKNOWLEDGMENTS

This work was supported by DFG, BMBF, GSI. We thank L.P. Csernai, M. Gyulassy, I.N. Mishustin, D.H. Rischke, and L. Satarov for numerous interesting discussions. A.D. acknowledges support from the DOE Research Grant, Contract No. De-FG-02-93ER-40764.

[1] J.C. Collins and M.J. Perry, Phys. Rev. Lett. **34**, 1353 (1975); E.V. Shuryak, Phys. Rept. **61**,

71 (1980); E. Witten, Phys. Rev. **D30**, 272 (1984); L. McLerran, Rev. Mod. Phys. **58**, 1021 (1986); J. Cleymans, R.V. Gavai, and E. Suhonen, Phys. Rept. **130**, 217 (1986).

[2] W. Scheid, H. Müller, and W. Greiner, Phys. Rev. Lett. **32**, 741 (1974); J. Hofmann, H. Stöcker, U. Heinz, W. Scheid, and W. Greiner, Phys. Rev. Lett. **36**, 88 (1976).

[3] H. Stöcker and W. Greiner, Phys. Rept. **137**, 277 (1986).

[4] R.B. Clare and D. Strottman, Phys. Rept. **141**, 177 (1986); B. Waldhauser, D.H. Rischke, U. Katscher, J.A. Maruhn, H. Stöcker, and W. Greiner, Z. Phys. **C54**, 459 (1992); N. Arbex, U. Ornik, M. Plümer, and R. Weiner, Phys. Rev. **C55**, 860 (1997).

[5] N.S. Amelin, E.F. Staubo, L.P. Csernai, V.D. Toneev, K.K. Gudima, and D. Strottman, Phys. Rev. Lett. **67**, 1523 (1991); L.V. Bravina, L.P. Csernai, P. Levai, and D. Strottman, Phys. Rev. **C50**, 2161 (1994); L.V. Bravina, Phys. Lett. **B344**, 49 (1995).

[6] D.H. Rischke, Y. Pürsün, J.A. Maruhn, H. Stöcker, and W. Greiner, Heavy Ion Phys. **1**, 309 (1995).

[7] C.M. Hung and E.V. Shuryak: Phys. Rev. Lett. **75**, 4003 (1995).

[8] J. Barrette *et al.* (E814 Collaboration), Phys. Rev. Lett. **73**, 2532 (1994); J. Barrette *et al.* (E877 Collaboration), Phys. Rev. **C55**, 1420 (1997); **C56**, 3254 (1997); W. Reisdorf and H.G. Ritter, Ann. Rev. Nucl. Part. Sci. **47**, 663 (1997); J.L. Chance *et al.* (EOS Collaboration), Phys. Rev. Lett. **78**, 2535 (1997); H. Liu *et al.* (E895 Collaboration), Nucl. Phys. **A638**, 451c (1998).

[9] K.G. Doss *et al.*, Phys. Rev. Lett. **57**, 302 (1986); K.H. Kampert, J. Phys. **G15**, 691 (1989); H.H. Gutbrod, A.M. Poskanzer, and H.G. Ritter, Rept. Prog. Phys. **52**, 1267 (1989).

[10] H. Appelshäuser *et al.* (NA49 Collaboration), Phys. Rev. Lett. **80**, 4136 (1998); M.M. Aggarwal *et al.* (WA98 Collaboration), nucl-ex/9807004 (subm. to Phys. Rev. Lett.); Nucl. Phys. **A638**, 459c (1998).

[11] V. Blobel et al., Nucl. Phys. **B69**, 454 (1974).

[12] I.N. Mishustin, V.N. Russkikh, and L.M. Satarov, Sov. J. Nucl. Phys. **48**, 454 (1988); Nucl. Phys. **A494**, 595 (1989); Sov. J. Nucl. Phys. **52**, 264 (1990); **54**, 459 (1991).

[13] J. Brachmann, A. Dumitru, J.A. Maruhn, H. Stöcker, W. Greiner, and D.H. Rischke, Nucl. Phys. **A619**, 391 (1997).

[14] A. Dumitru, U. Katscher, J.A. Maruhn, H. Stöcker, W. Greiner, and D.H. Rischke, Phys. Rev. **C51**, 2166 (1995); Z. Phys. **A353**, 187 (1995).

[15] B.D. Serot and J.D. Walecka, Adv. Nucl. Phys. **16**, 1 (1986); D.H. Rischke, Y. Pürsün, and

J.A. Maruhn, Nucl. Phys. **A595**, 383 (1995).

[16] A. Chodos, R.L. Jaffe, K. Johnson, C.B. Thorn, and V. Weisskopf, Phys. Rev. **D9**, 3471 (1974).

[17] D.H. Rischke and M. Gyulassy, Nucl. Phys. **A608**, 479 (1996).

[18] M. Reiter, A. Dumitru, J. Brachmann, J.A. Maruhn, H. Stöcker, and W. Greiner, Nucl. Phys. **A643**, 99 (1998).

[19] H. Sorge, Phys. Rev. Lett. **78**, 2309 (1997); J.Y. Ollitrault, Nucl. Phys. **A638**, 195c (1998); P. Danielewicz, R.A. Lacey, P.B. Gossiaux, C. Pinkenburg, P. Chung, J.M. Alexander, and R.L. McGrath, Phys. Rev. Lett. **81**, 2438 (1998); S. Soff, S.A. Bass, M. Bleicher, H. Stöcker, and W. Greiner, nucl-th/9903061; P.K. Sahu, W. Cassing, U. Mosel, and A. Ohnishi, nucl-th/9907002.

[20] P. Danielewicz and G. Odyniec, Phys. Lett. **B157**, 146 (1985).

[21] H. Liu, S. Panitkin, and N. Xu, Phys. Rev. **C59**, 348 (1999).

[22] B. Li and C.M. Ko, Phys. Rev. **C58**, R1382 (1998).

[23] L. Csernai and D. Röhricht, Phys. Lett. **B458**, 454 (1999).

[24] J. Brachmann, S. Soff, A. Dumitru, H. Stöcker, J.A. Maruhn, W. Greiner, D.H. Rischke, and L.V. Bravina, nucl-th/9908010.

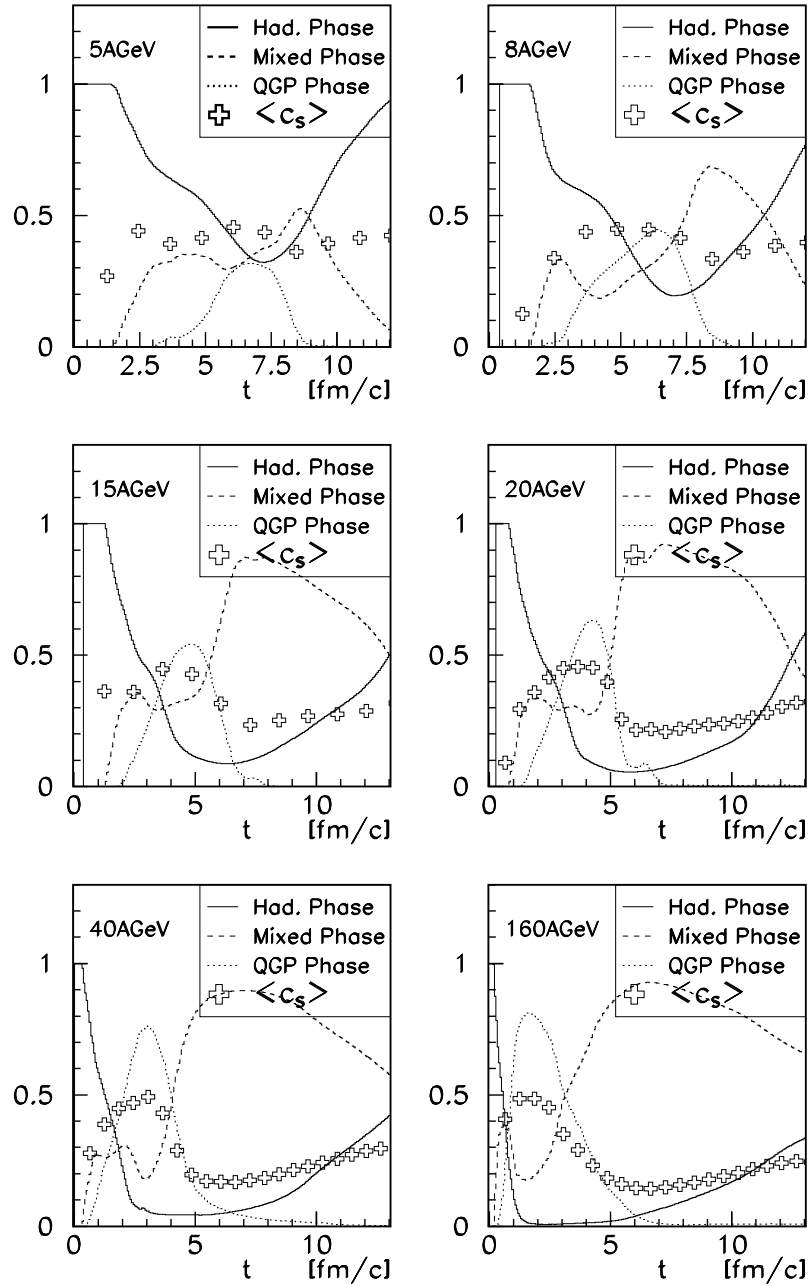


FIG. 1. Evolution of the isentropic speed of sound and the fraction of baryon charge in the various phases; Pb+Pb collisions at $b = 3$ fm.

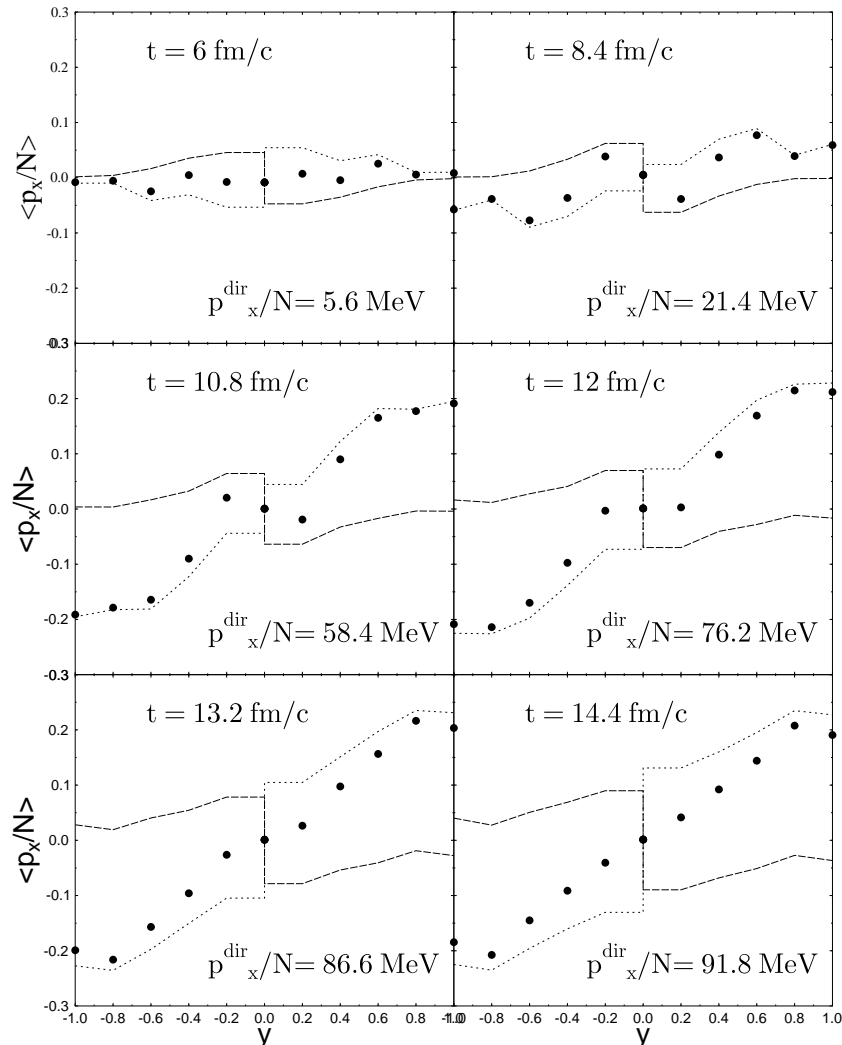


FIG. 2. Mean in-plane transverse momentum per nucleon in $\text{Pb}(2A \text{ GeV})+\text{Pb}$ collision at $b = 3$ fm. Dotted and dashed lines show the flow and antiflow, respectively, dots represent the sum (the net flow).

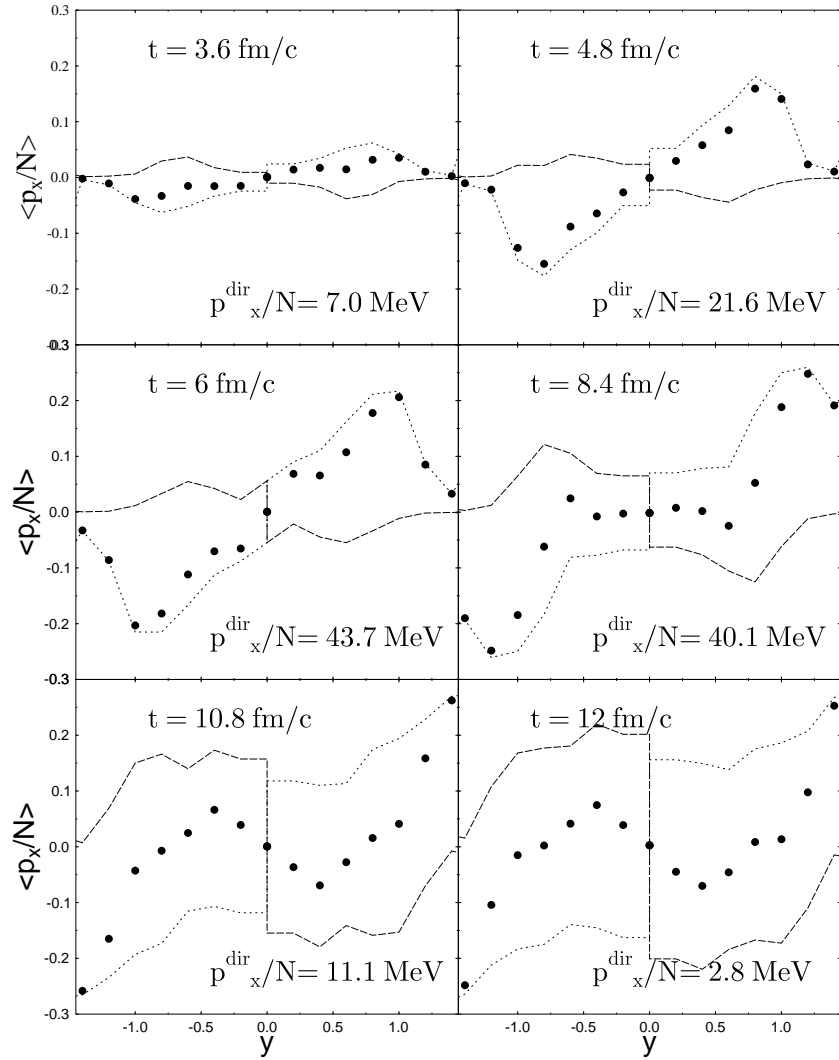


FIG. 3. As in Fig. 2 but for $E_{Lab}^{kin} = 8A$ GeV.

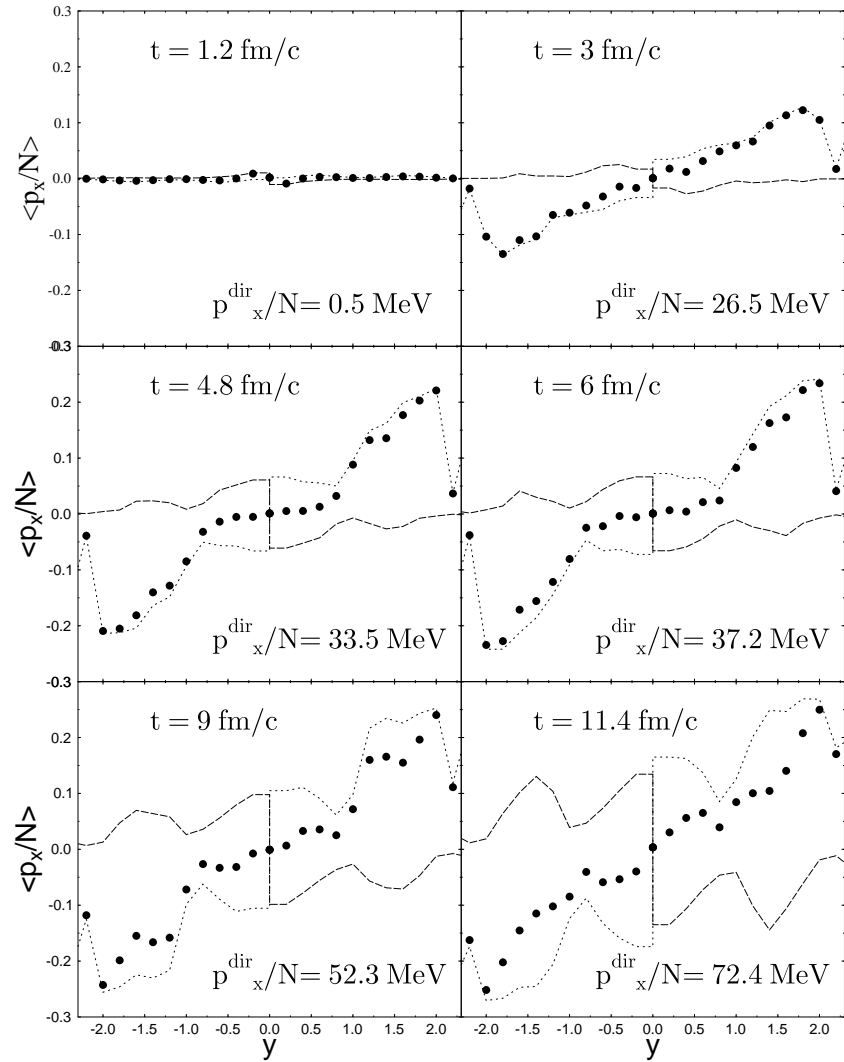


FIG. 4. As in Fig. 2 but for $E_{Lab}^{kin} = 40A$ GeV.